Acta Chemica Scandinavica, 1998: 52: 154–159
Printed in UK – all rights reserved

ACTA
CHEMICA SCANDINAVICA
ISSN 0904-213X

Radical Reactivity of Radical Ions in Solution. Radical–Radical and Radical–Substrate Coupling Mechanisms

Vernon D. Parker

Department of Chemistry and Biochemistry, Utah State University, Logan, Utah 84322-0300, USA

Dedicated to Professor Lennart Eberson on the occasion of his 65th birthday

Parker, V. D., 1998. Radical Reactivity of Radical Ions in Solution. Radical–Radical and Radical–Substrate Coupling Mechanisms. – Acta Chem. Scand. 52: 154–159. © Acta Chemica Scandinavica 1998.

The linear sweep voltammetry response to competitive radical ion–substrate coupling and radical ion dimerization mechanisms was determined by digital simulation. The simulations were carried out to mimic the conditions under which experimental studies had previously shown that the radical ion–substrate coupling mechanism is the preferred reaction pathway. It was observed that in order for the dependence of the peak potential on substrate concentration ($\Delta E^p/\Delta \log C_A$) to be in the experimentally observed range (36–40 mV/decade) that the relative rate constants for radical ion–substrate coupling and radical ion dimerization (k_i/k_{ii}) must be greater than about 10. It is pointed out that since the reactants, the transition states and the products differ by only a single electron that these competitive reactions represent an ideal test case for the configuration mixing (CM) model. The CM model predicts an electronic reaction barrier for reaction (i) but not for reaction (ii). The difference in standard free energy changes for reactions (i) and (ii) were estimated to be of the order of 7 kcal mol^{-1} or greater with (ii) being energetically more favorable than (i). It is concluded that the experimental data for the relative rates of reactions (i) and (ii) do not conform to the CM model predictions in the cases discussed.

$$ArH^{\cdot+} + ArH \rightarrow {}^{+}ArH\text{–}ArH^{\cdot} \quad \text{(i)}$$

$$ArH^{\cdot+} + ArH^{\cdot+} \rightarrow {}^{+}ArH\text{–}ArH^{+} \quad \text{(ii)}$$

There has been considerable discussion of radical ion reactivity over the past fifteen years, mostly dealing with the polar reactivity of radical cations toward nucleophiles.[1–18] Despite the extensive discussion, which has included the applicability of the configuration mixing (CM) model to estimate barriers for these reactions, there still does not appear to be general agreement on the factors which influence the reactivity of radical ions.

During the early 1980s the results of a number of studies dealing with one aspect of radical ion reactivity, the factors influencing which of the dimer forming mechanisms of radical ions is favored, were reported.[19–25] These mechanisms include radical ion dimerization (radical–radical coupling) and radical ion–substrate (radical–substrate) coupling and are illustrated in Schemes 1 and 2, respectively.

$$A + e^- \rightleftharpoons B \quad (1)$$

$$2\,B \rightarrow \text{Products} \ (k_2) \quad (2)$$

Scheme 1.

$$A + e^- \rightleftharpoons B \quad (3)$$

$$B + A \rightleftharpoons A\text{–}B \quad (k_4, k_{-4}) \quad (4)$$

$$A\text{–}B + B \rightarrow \text{Products} \quad (k_5) \quad (5)$$

Scheme 2.

The purpose of this paper is to show the significance of the observation of kinetics consistent with the radical–substrate coupling mechanism in terms of the relative barriers of radical–radical and radical–substrate coupling. This is accomplished by presenting theoretical linear sweep voltammetry (LSV) data under conditions where the two mechanisms compete with each other to determine the minimum value of k_4/k_2 consistent with experimental data reported earlier.[19–25] This approach is made possible by the fact that the LSV response to the two mechanisms is radically different. The calculations are guided by the earlier experimental data which were presented to show that the radical–substrate mechanism

is the favored reaction pathway for a number of radical ion dimer forming reactions.

Results

Theoretical LSV relationships for radical ion dimer forming reactions. The voltage sweep rate (v) and the substrate concentration (C_A) are the experimental variables for LSV mechanism analysis of reactions taking place at electrodes. The LSV slopes, $\Delta E^p/\Delta \log v$ and $\Delta E^p/\Delta \log C_A$ where ΔE^p is the change in peak potential, can be derived from the rate law for a mechanism and are described by eqns. (6) and (7), where a and b are the reaction orders in A and B, respectively.[26] At 25 °C ln 10 (RT/F) is equal to 59.2 mV. The rate law for irreversible dimerization (Scheme 1) is given by eqn. (8). The steady state derived rate law for radical–substrate coupling (9) has two limiting cases, (10) and (11), depending on which term in the denominator of rate law (9) is the larger of the two.

$$\Delta E^p/\Delta \log v = \ln 10(RT/F)/(b+1) \quad (6)$$

$$\Delta E^p/\Delta \log C_A = (a+b-1)\ln 10(RT/F)/(b+1) \quad (7)$$

$$-dC_B/dt = k_2 C_B^2$$

$$(\Delta E^p/\Delta \log C_A = 19.7 \text{ mV/decade at } 25\,^\circ\text{C}) \quad (8)$$

$$-dC_B/dt = k_5 k_4 C_B^2 C_A/(k_{-4} + k_5 C_B) \quad (9)$$

$$-dC_B/dt = k_5 K_4 C_B^2 C_A$$

$$(\Delta E^p/\Delta \log C_A = 39.4 \text{ mV/decade at } 25\,^\circ\text{C}) \quad (10)$$

$$-dC_B/dt = k_4 C_B C_A$$

$$(\Delta E^p/\Delta \log C_A = 29.6 \text{ mV/decade at } 25\,^\circ\text{C}) \quad (11)$$

The dependence of the peak potential on the voltage sweep rate, $\Delta E^p/\Delta \log v$, does not distinguish between the mechanisms, since for rate laws (8) and (10) the reaction order in B (b) has the same value, and the slope is equal to 19.7 mV/decade (at 25 °C) in both cases. On the other hand, $\Delta E^p/\Delta \log C_A$ is significantly different for the radical–radical coupling mechanism (Scheme 1) and both limiting cases of the radical–substrate coupling mechanism (Scheme 2). The values of $\Delta E^p/\Delta \log C_A$ derived using eqn. (7) are given in parentheses after the rate laws in all cases where (7) is applicable (the sign of $\Delta E^p/\Delta \log C_A$ is positive for reduction processes and negative for oxidation processes). The exception is rate law (9), which predicts that the effect of b will vary depending upon the relative magnitudes of the terms in the denominator.

Theoretical LSV data for rate law (9). The magnitude of $\Delta E^p/\Delta \log C_A$ reported for radical–substrate coupling reactions has varied from 33.4 to 40.3 mV/decade with an average value close to 37 mV/decade. The latter suggests that neither limiting case (10) nor (11), for which the theoretical values can be deduced using eqn. (7), apply to the experimental data which are available.[20–25] The experimental data are for v ranging from 100 to 400 mV/s and C_A ranging from 0.5 to 2.0 mM.

Theoretical LSV data for the radical–substrate coupling mechanism under non-limiting conditions were obtained by digital simulation. Recent advances in digital simulation of electrode processes[27–29] have resulted in an algorithm suitable for the simulation of complex and competitive electrode mechanisms. It is feasible, using the Rudolph method, to analyze not only the radical–substrate coupling mechanism but also competitive radical–substrate and radical–radical coupling mechanisms. The theoretical data in Table 1 are for simulations of the radical–substrate coupling mechanism with a range of rate constants expected to encompass those encountered in experimental studies. In the simulations, v was held at 100 mV/s and C_A was varied from 0.5 to 2.0 mM in order to obtain theoretical data using simulation variables in the range of the experimental variables used in the mechanism studies.[19–25] It was estimated from the published experimental data that k_4 for these reactions are in the range from 10^6 to 10^8 M^{-1} s^{-1}. For these values of k_4, k_{-4} and k_5 were varied to find the values consistent with the experimental $\Delta E^p/\Delta \log C_A$, about 37 mV/decade. The magnitude of $\Delta E^p/\Delta \log C_A$ depends upon all three rate constants, and there do not appear to be any trends in the data that can be attributed to any one of the rate constants alone.

Theoretical LSV data for competing radical–substrate and radical–radical coupling reactions. The data in Table 1 were used to select conditions for simulation of the competing mechanisms. The value of k_5 was set at 10^8 M^{-1} s^{-1}, and several series of simulations were carried out with k_4 equal to 10^6, 10^7 and 10^8 M^{-1} s^{-1} with K_4 equal to either 10 or 10^2 M^{-1}, while k_2 was varied from 10^4 to 10^7 M^{-1} s^{-1}. The last column in Table 2 gives the value of $(k_4/k_2)_{min}$ defined as the minimum value of the rate constant ratio necessary for $\Delta E^p/\Delta \log C_A$ to be about 37.4 mV/decade. The simulations were tested by variation of the resolution of the simulations. Digisim 2.0, the program[30] used for the simulations, has three variable model parameters which affect the accuracy of the simulation. The parameters include: (i) the potential step width (ΔE), (ii) the exponential grid factor (β) and (iii) the number of iterations (n). The three parameters were varied sequentially over a factor of at least 10 ($\Delta E = 0.01$–1 mV); $\beta = 0.05$–0.5; $n = 1$–10) while holding all other variables constant. No changes in E^p were observed over the entire range of model parameters, indicating that the results are a true reflection of the LSV response to the competitive mechanisms simulated.

Discussion

The existence of two mechanisms, the compositions of the reactants, products and transition states which differ by only a single electron, represents a highly unique

Table 1. Theoretical LSV data for the radical–substrate coupling mechanism.[a]

		$\Delta E^p/\Delta \log C_A$ (mV/decade) when $k_5/M^{-1}s^{-1}$ equals:			
$k_4/M^{-1}s^{-1}$	$k_{-4}/M^{-1}s^{-1}$	10^7	10^8	10^9	10^{10}
10^6	10^6	35.9	38.4	38.4	38.4
	10^5	38.5	38.4	36.4	32.1
	10^4	38.4	36.0	32.2	32.1
	10^3	35.4	35.2	30.1	29.7
10^7	10^7	36.0	38.7	39.2	39.2
	10^6	38.7	39.2	39.2	37.9
	10^5	39.5	39.4	37.7	34.4
	10^4	41.0	37.5	33.7	30.7
10^8	10^8	36.0	38.7	39.2	39.4
	10^7	38.7	39.2	39.4	39.4
	10^6	39.9	40.2	39.9	38.9

[a]Voltage sweep rate 0.1 V s^{-1}, C_A ranging from 0.5 to 2.0 mM, simulation at 0.1 mV/time step using Digisim 2.0.[30]

Table 2. Theoretical LSV data for competitive radical–radical and radical–substrate coupling mechanisms.[a]

		$\Delta E^p/\Delta \log C_A$ (mV/decade) when $k_2/M^{-1}s^{-1}$ equals:				
$k_4/M^{-1}s^{-1}$	$k_{-4}/M^{-1}s^{-1}$	10^4	10^5	10^6	10^7	$(k_4/k_2)_{min}$
10^6	10^5	37.0	28.7	21.1	20.7	10^2
	10^4	38.2	36.9	27.4	24.6	10
10^7	10^6	39.0	37.7	28.7	20.9	10^2
	10^5	39.4	39.2	38.0	28.4	10
10^8	10^7	39.2	37.9	28.9	21.1	10^3
	10^6	40.2	40.0	38.9	29.4	10^2

[a]Voltage sweep rate 0.1 V s^{-1}, C_A ranging from 0.5 to 2.0 mM, $k_5 = 10^8$ $M^{-1}s^{-1}$, simulation at 0.1 mV/time step using Digisim 2.0.[30]

situation. The difference in free energy changes for the two reactions can readily be estimated from the difference in electrode potentials for the one-electron charge-transfer reactions connecting the two product states and that connecting the two reactant states. Estimation of the difference in free energies of activation for the two processes requires only a reliable estimate of the relative rate constants.

The scenario described in the previous paragraph represents the situation for competitive radical ion dimerization and radical ion–substrate coupling mechanisms. Since reactants, transition states, and products for the two processes differ by only a single electron, steric factors should be the same for both pathways and we would expect that the partitioning between the two mechanisms to be governed primarily by electronic factors. This would appear to be an ideal situation for testing any theory which can be offered for the estimation of electronic reaction barriers for radical ion reactions.

Application of the configuration mixing model. The CM model has been applied to the estimation of reaction barriers of radical cation–nucleophile combination reactions.[7] The essence of the application of the model is that an initial gap (IG), which corresponds to a vertical transition of the reactant state to an excited state with a valence bond configuration common to the product state, is estimated. For example, the IG for the cation–anion combination reaction (12) is equal to the vertical electron affinity of R^+ plus the vertical ionization potential of X^- in solution. On the other hand, there is no CM IG for the free radical dimerization reaction (13), since the reactant radical pair ground-state configuration ($R \cdot\cdot R$) is also a ground-state product configuration. In the case of radical cation–nucleophile combination reactions (14), the first excited state configuration resulting from a single electron shift between radical cation and nucleophile does not correspond to a ground-state product configuration, but ($^{\cdot}ArH \cdot\cdot Nu^+$) is reached by an additional excitation, a singlet–triplet transition of the neutral substrate (radical cation precursor).

$$R^+ + X^- \rightarrow R\text{–}X \quad (12)$$

$$2\,R^{\cdot} \rightarrow R\text{–}R \quad (13)$$

$$ArH^{\cdot +} + Nu: \rightarrow {}^{\cdot}ArH\text{–}Nu^+ \quad (14)$$

The reactions which must be considered for competitive dimer-forming reactions of radical cations are (15) and (16). The radical cation dimerization (15), like the free radical dimerization, is not associated with a CM IG since the ground-state reactant pair configuration ($^+ArH \cdot\cdot ArH^+$) is also a ground-state product configuration. Electronically, the radical cation–substrate coupling reaction appears to be very similar to the radical

cation–nucleophile combination reaction. However, a single electron shift from substrate to radical cation is degenerate and does not give a change in configuration. Consequently, the CM IG for reaction (16) is simply a singlet–triplet transition to the product ground-state configuration ($^{\cdot}ArH\cdot\cdot ArH^{+}$). Thus, the CM model predicts that radical cation dimerization will not have an electronic barrier, while that for radical cation–substrate coupling will be significant.

$$2\,ArH^{\cdot+} \rightarrow {}^{+}ArH\text{–}ArH^{+} \qquad (15)$$

$$ArH^{\cdot+} + ArH \rightarrow {}^{\cdot}ArH\text{–}ArH^{+} \qquad (16)$$

Singlet–triplet excitation energies for aromatic compounds range from about 40 to about 90 kcal mol^{-1}.[31] The singlet–triplet energies of the aromatic precursors of the radical cations known to undergo radical cation–substrate coupling reactions (**1** and **2**) are not known. However, comparing the structures of these compounds with those having known singlet–triplet energies suggests mid-range values of the order of 60–80 kcal mol^{-1} as rough estimates.

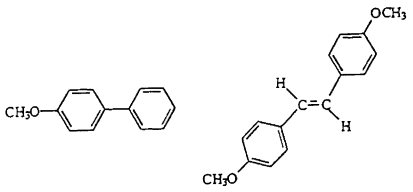

1 2

A characteristic of reactions (14) and (16) is that the free-radical products are more easily oxidized than the neutral ArH and the initial adduct formation is followed by further electron transfer to give $^{+}ArH\text{–}Nu^{+}$ and $^{+}ArH\text{–}ArH^{+}$, respectively. This means that E°_{17} is expected to be more positive than E°_{18}. The differences in free energies of reactions (15) and (16) can be calculated from the electrode potential difference as in eqn. (19). In the cases where electrode potentials for charge-transfer reactions of free radicals resulting from adduct forming reactions of radical anions[32] and radical cations[33] have been determined, these processes take place at potentials greater than 300 mV more positive or 300 mV more negative, respectively, than the corresponding charge-transfer reaction of the neutral substrates. Therefore, we conclude that the minimum value of the free energy difference $(\Delta G^{\circ}_{16} - \Delta G^{\circ}_{15})_{min}$ is of the order of 7 kcal mol^{-1}.

$$ArH^{\cdot+} + e^{-} \rightleftharpoons ArH \qquad (17)$$

$$^{+}ArH\text{–}ArH^{+} + e^{-} \rightleftharpoons {}^{\cdot}ArH\text{–}ArH^{+} \qquad (18)$$

$$\Delta G^{\circ}_{16} - \Delta G^{\circ}_{15} = F(E^{\circ}_{17} - E^{\circ}_{18}) \qquad (19)$$

The last column in Table 2 gives the minimum values of the relative rate constants for radical–substrate and radical–radical coupling for $\Delta E^{p}/\Delta \log C_A$ to fall within the range of 37 ± 2 mV under the experimental conditions reported.[19–25] Applying this to the specific case of competitive radical cation coupling reactions (15) and (16) we find that $(k_{16}/k_{15})_{min}$ must be greater than 10–100 to fulfil this condition. This means that the reaction barrier for dimerization reaction (15) is somewhat greater than that for radical cation–substrate coupling reaction (16).

In terms of the CM model analysis of these two reactions, we are forced to conclude that even though reaction (15) is thermodynamically more favorable than reaction (16) by about 7 kcal mol^{-1} and reaction (16) is predicted by the model to have a significant barrier while reaction (15) is not, reaction (16) is observed to be the favored pathway for the radical cations derived from **1** and **2**.

Factors influencing dimer-forming reaction pathways of radical ions. The radical cations of many aromatic compounds do not readily undergo either reaction (15) or reaction (16). The structural feature of the radical cations of **1** and **2** that promotes these reactions is the presence of the methoxy substituents. We attribute the substituent effect to the separation of charge and radical centers, as depicted by the resonance form (**3**). This gives rise to an enhanced radical reactivity. A pertinent example which supports this interpretation can be found in the fact that the anthracene radical anion **4** is persistent in aprotic solvents in the absence of proton donors while 9-nitroanthracene radical anion **5** rapidly dimerizes.[34,35]

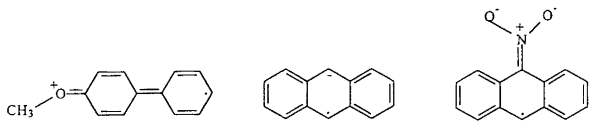

3 4 5

Radical–substrate coupling of 4-methoxystyrene radical cation. The electrochemical oxidations of **2** and the related compound 4-methoxystyrene (MS) result in the formation of dimeric compounds which result from an initial coupling reaction followed by cyclization and proton loss.[36] Laser flash photolysis studies[37] of the oxidation of MS in acetonitrile revealed that the initial step of the dimerization–cyclization reactions under these conditions is the coupling between radical cation and substrate with a second-order rate constant of 1.4×10^{9} M^{-1} s^{-1}. Unfortunately, it is not possible to study this reaction by LSV, since severe product adsorption on the electrode precludes quantitative studies.[36] However, the photochemical study[37] gives a direct example of a low-barrier radical–substrate coupling reaction which is predicted by the CM model to have a substantial reaction barrier.

An alternative mechanistic interpretation of rate law (10). It has recently been pointed out that the observation of rate law (10) can also be consistent with the radical ion

Table 2. Theoretical LSV data for competitive radical–radical and radical–substrate coupling mechanisms.[a]

		$\Delta E^p/\Delta \log C_A$ (mV/decade) when k_2 / $M^{-1} s^{-1}$ equals:				
k_4 / $M^{-1} s^{-1}$	k_{-4} / $M^{-1} s^{-1}$	10^4	10^5	10^6	10^7	$(k_4/k_2)_{min}$
10^6	10^5	37.0	28.7	21.1	20.7	10^2
	10^4	38.2	36.9	27.4	24.6	10
10^7	10^6	39.0	37.7	28.7	20.9	10^2
	10^5	39.4	39.2	38.0	28.4	10
10^8	10^7	39.2	37.9	28.9	21.1	10^3
	10^6	40.2	40.0	38.9	29.4	10^2

[a]Voltage sweep rate 0.1 $V s^{-1}$, C_A ranging from 0.5 to 2.0 mM, $k_5 = 10^8$ $M^{-1} s^{-1}$, simulation at 0.1 mV/time step using Digisim 2.0.[30]

dimerization mechanism under certain conditions.[38] The mechanism (Scheme 3) involves reversible dimerization of the radical ion (B) followed by reaction with the substrate (A). The product forming reaction in this mechanism most often involves proton transfer with A acting either as a base (B is a radical cation) or as an acid (B is a radical anion).

$$2\,B \rightleftharpoons C \qquad (20)$$

$$C + A \rightarrow \text{Products} \qquad (21)$$

Scheme 3.

We can briefly consider two specific cases where we have observed rate law (10) for reactions of radical cations[23] and for radical anions[25] in the light of the mechanism shown in Scheme 3. The radical cation case requires that neutral 4-methoxybiphenyl (**1**) should act as a base even though the solvent, acetonitrile, is a much stronger base and present in concentrations 10^4 times as great as (**1**). For the other case we can examine the data for the dimer-forming reactions of isobutylene Meldrum's acid (**6**) anion radical. The substrate concentration dependence $\Delta E^p/\Delta C_A$ was observed to be equal to 39.4 ± 0.9 mV/decade for the reaction in DMF containing water (280 mM). In order for this mechanism (Scheme 3) to account for the data, the substrate is required to act as base even under conditions where the water concentration is of the order of 300 times as great as that of **6**. The substrate **6** has no acidic hydrogens in spite of the common name. The parent compound in this series, Meldrum's acid (**7**), is acidic ($pK_a = 7.3$ in DMSO) by virtue of the methylene group situated between the two carbonyl groups. The obvious conclusion is that neither **1** nor **6** is likely to act as a proton acceptor or donor under the conditions reported. Therefore, it is highly unlikely that the mechanism in Scheme 3 plays an important role in the radical ion dimer-forming reactions of these substrates.

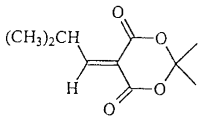

6

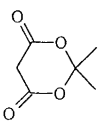

7

Conclusions

The alternative mechanisms for radical ion dimer-forming reactions, radical ion dimerization and radical ion–substrate coupling, provide a unique opportunity to test the application of the CM model for estimating reaction barriers. Since the reactants, transition states, and products of the two reaction pathways differ by only a single electron, the difference in reaction barriers for the two reactions is expected to depend primarily on electronic factors. The CM model takes into account only electronic factors. The CM model predicts a significant barrier for the radical ion–substrate coupling reaction but not for radical ion dimerization. In the cases discussed here the opposite result is observed experimentally: the radical ion–substrate mechanism is the preferred pathway. This is not to say that the radical–substrate coupling mechanism is always, or even usually, the preferred reaction pathway but that it is in some cases. The overall conclusion is obvious: the CM model does not give reliable estimates of reaction barriers for radical ion reactions.

Acknowledgement. Financial support from the National Science Foundation (Grant CHE-9708935) is gratefully acknowledged.

References

1. Parker, V. D. *Acc. Chem. Res. 17* (1984) 243.
2. Eberson, L., Blum, Z., Helgée, B. and Nyberg, K. *Tetrahedron 34* (1978) 731.
3. Szwarc, M. and Jagur-Grodzinski, J. In: Szwarc, M., Ed., *Ions and Ion Pairs in Organic Reactions*, Wiley, New York 1974, Vol. 2, Chap. 1.
4. Jensen, B. S. and Parker, V. D. *J. Am. Chem. Soc. 97* (1975) 5211.
5. Pross, A. *J. Am. Chem. Soc. 108* (1986) 3537.
6. Parker, V. D. and Tilset, M. *J. Am. Chem. Soc. 109* (1987) 2521.
7. Shaik, S. S. and Pross, A. *J. Am. Chem. Soc. 111* (1989) 4306.
8. Reitstöen, B., Norrsell, F. and Parker, V. D. *J. Am. Chem. Soc. 111* (1989) 8463.

9. Parker, V. D., Reitstöen, B. and Tilset, M. *J. Phys. Org. Chem. 2* (1989) 580.
10. Reitstöen, B. and Parker, V. D. *J. Am. Chem. Soc. 112* (1990) 4968.
11. Reitstöen, B. and Parker, V. D. *J. Am. Chem. Soc. 113* (1991) 6954.
12. Parker, V. D., Handoo, K. L. and Reitstöen, B. *J. Am. Chem. Soc. 113* (1991) 6218.
13. Parker, V. D. and Tilset, M. *J. Am. Chem. Soc. 113* (1991) 8778.
14. Bethell, D. and Parker, V. D. *J. Phys. Org. Chem. 5* (1992) 317.
15. Reitstöen, B. and Parker, V. D. *Acta Chem. Scand. 46* (1992) 464.
16. Parker, V. D., Pedersen, M. and Reitstöen, B. *Acta Chem. Scand. 47* (1993) 560.
17. Parker, V. D., Handoo, K. L. and Norrsell, F. *J. Org. Chem. 58* (1993) 4929.
18. Workentin, M., Johnston, L. J., Wayner, D. D. M. and Parker, V. D. *J. Am. Chem. Soc. 116* (1994) 8279.
19. Parker, V. D. *Acta Chem. Scand., Ser. B 35* (1981) 147.
20. Parker, V. D. *Acta Chem. Scand., Ser. B 35* (1981) 149.
21. Parker, V. D. *Acta Chem. Scand., Ser. B 35* (1981) 279.
22. Aalstad, B., Ronlan, A. and Parker, V. D. *Acta Chem. Scand., Ser. B 35* (1981) 247.
23. Aalstad, B., Ronlan, A. and Parker, V. D. *Acta Chem. Scand., Ser. B 35* (1981) 649.
24. Margaretha, P. and Parker, V. D. *Acta Chem. Scand., Ser. B 36* (1981) 260.
25. Margaretha, P. and Parker, V. D. *Chem. Lett.* (1984) 681.
26. Parker, V. D. *Acta Chem. Scand., Ser. B 36* (1981) 259.
27. Rudolph, M. *J. Electroanal. Chem. 314* (1991) 13.
28. Rudolph, M. J. *Electroanal. Chem. 338* (1992) 85.
29. Rudolph, M. In: Rubinstein, I., Ed., *Physical Chemistry: Principles, Methods and Applications*, Marcel Dekker, New York 1993.
30. Rudolph, M., Reddy, D. P. and Feldberg, S. W. *Anal. Chem. 66* (1994) 589 A; Digisim 2.0 program available from BioAnalytical Systems Inc., 2701 Kent Ave., W. Lafayette, IN 47906.
31. McGlynn, S. P., Azumi, T. and Kinoshita, M. *The Triplet State*, Prentice-Hall, New Jersey 1969.
32. Parker, V. D., Tilset, M. and Hammerich, O. *J. Am. Chem. Soc. 109* (1987) 7905.
33. Hammerich, O. and Parker, V. D. *J. Am. Chem. Soc. 96* (1974) 4289.
34. Hammerich, O. and Parker, V. D. *Acta Chem. Scand., Ser. B 35* (1984) 341.
35. Hammerich, O. and Parker, V. D. *Acta Chem. Scand., Ser. B 37* (1983) 379.
36. Parker, V. D. and Eberson, L. *Acta Chem. Scand. 24* (1970) 3553.
37. Schepp, N. P. and Johnston, L. J. *J. Amer. Chem. Soc. 116* (1994) 6895.
38. Andersen, M. L., Nielsen, M. F. and Hammerich, O. *Acta Chem. Scand. 51* (1997) 94.

Received February 24, 1997.